J Bioenerg Biomembr (2014) 46:357–370
DOI 10.1007/s10863-014-9563-y

I - insulin transfer to mitochondria

María del Carmen Camberos · Gabriel Cao · María I. Wanderley · Daniel P. Udrisar · Juan C. Cresto

Received: 11 April 2014 / Accepted: 2 July 2014 / Published online: 8 August 2014

Abstract The aim of this study was to determine if insulin is transferred to mitoplasts by insulin-degrading enzyme (IDE).

Hepatic mitochondria were isolated and controlled by electron microscopy. IDE was obtained from rats muscle by successive chromatography steps. Insulin accumulation in mitoplasts and outer membrane + intermembrane space (OM + IMS) was studied with ^{125}I-insulin. Mitochondrial insulin accumulation and degradation was assayed with Sephadex G50 chromatography, insulin antibody and 5 % TCA. Mitoplasts and OM + IMS were isolated with digitonin. Insulin accumulation was studied at 25 °C at different times, without or with IDE, Bacitracin, 2,4-dinitrophenol, apyrase or sodium succinate + adenosine diphosphate. Insulin accumulation in mitoplasts and OM + IMS after mitochondrial cross-linking was studied with electrophoresis in SDS-PAGE, immunoblots of IDE, insulin or TIM23 (inner mitochondrial transporter) and autoradiography.

The studies showed that addition of IDE increased insulin transfer from OM + IMS to mitoplasts, and the insulin accumulation in mitoplast was IDE dependent. Bacitracin and 2,4-dinitrophenol decreased this transfer. The [Insulin-IDE] complex and [Mitoplasts] was studied as a bimolecular reaction following a second order reaction. The constant "*k*" (liter.mol^{-1} s^{-1}) showed that IDE increased and Bacitracin or 2,4-dinitrophenol decreased the velocity of insulin transfer. SDS-PAGE and immunoblots studies showed bands and radioactivity coincident with IDE, insulin and TIM23. Non degraded insulin was demonstrated in immunoblot after IDE immunoprecipitation from mitoplasts. Confocal studies showed mitochondrial colocalization of IDE and insulin.

The results showed that insulin at 25 °C were transferred from OM + IMS to mitoplasts by IDE or that the enzyme facilitates this transfer, and they reach the matrix together.

Keywords IDE-Insulin transfer · Transfer kinetics · Insulin-IDE cross-linking · Insulin-IDE confocal studies · Degradation assay

Abbreviations

IDE	Insulin-degrading enzyme
M	mitoplasts
OM	outer membrane
IMS	inter-membrane space
IM	inner membrane
Mx	matrix
OM + IMS	outer membrane + inter-membrane space
DNP	2,4-dinitrophenol
NEM	N-ethylmaleimide
TIM23	inner mitochondrial transporter protein

Introduction

Liver cells have many metabolic functions in relation to carbohydrates, lipids, triglycerides, cholesterol, bile secretion,

Electronic supplementary material The online version of this article (doi:10.1007/s10863-014-9563-y) contains supplementary material, which is available to authorized users.

M. del Carmen Camberos · J. C. Cresto (✉)
Endocrinology Research Center (CEDIE-CONICET) Children Hospital "R. Gutiérrez", Gallo 1330, 1425 Ciudad de Buenos Aires, Argentina
e-mail: jcresto@cedie.org.ar

G. Cao
Pathology Division, Children Hospital "P. Elizalde", Buenos Aires, Argentina

M. I. Wanderley · D. P. Udrisar
Endocrinology and Metabolism Laboratory, Physiology and Pharmacology Department, University of Pernambuco, Recife, Pernambuco, Brazil

albumin synthesis and others (Guyton & Hall: Tratado de Fisiología Humana 1997). Moreover it accumulates and degrades polypeptide hormones like insulin where 50 % of it is degraded before reaching the circulation (Duckworth et al. 1998).

Hepatocytes constantly handle large amounts of insulin because pancreatic islets release it through the portal vein. Insulin is internalized for degradation as well as for other physiological processes, such as control of proteolysis and peroxisomal fatty acid oxidation (Hamel et al. 2001, Bennett et al. 1997). The interaction of insulin-degrading enzyme (IDE) with insulin regulates these functions, and substantial evidence exists suggesting that the primary cellular insulin-degrading activity is dependent on IDE. Although IDE was first described in cytosol, its sub-cellular localization has been demonstrated in various organelles, such as endosomes (Hamel et al. 1991), peroxisomes (Authier et al. 1995; Hamel et al. 2001), nucleus (Cesar Vieira et al. 2011), endoplasmic reticulum (Cesar Vieira et al. 2011), and mitochondria (Leissring et al. 2004).

The aforementioned functions of the liver cells require energy which depends on mitochondrial activity, partially controlled by insulin through the supply of mitochondrial substrates. Many proteins are translocated from cytosol to the mitochondria after hormone stimulation where they have direct activity. For example, tyrosine kinase A is translocated after the cyclic AMP was incremented by glucagon, and PKB/Akt was translocated to mitochondria through phosphoinositol-3-kinase cascade after insulin-receptor binding (Salvi et al. 2005; Hütemann et al. 2007). Direct mitochondrial control by internalized insulin, independent of the insulin receptor pathway, could be supported by some experimental results. Wortmannin, an inhibitor of phosphatidylinositide-3-kinases and its insulin pathway, did not inhibit mitochondrial insulin stimulation. It was demonstrated that insulin activates pyruvate dehydrogenase complex (PDHc) in mutant cells with receptor inactivated tyrosine kinase domain (Carusso et al. 2001; Wymann et al. 1996).

Insulin has been described inside the mitochondria in confocal studies directed to study SIRT4 interaction with mitochondrial glutamate dehydrogenase, but there was not mention about how the hormone arrived at the mitochondria (Haigis et al. 2006). Our objective was to investigate if IDE facilitates the insulin transfer to mitochondria because IDE is the main insulin binding protein after internalization (Duckworth et al. 1998).

Material and methods

Male Wistar rats (200–250 g) were purchased in Biochemistry, University of Buenos Aires (UBA) City of Buenos Aires, Argentina. Porcine insulin was provided by Dr. Anderson (Laboratorios Beta S.A., City of Buenos Aires, Argentina). $Na^{125}I$ (17.4 Ci/mg) was purchased in DuPont (Boston, MA, USA). DEAE-Sephadex A50, Sephadex G-25 and Sephadex G-50 Superfine came from Pharmacia Diagnostics AB (Uppsala, Sweden). Pentyl-Agarose, Dithiothreitol (DTT), N-ethylmaleimide (NEM), Bacitracin, 2,4-Dinitrophenol (DNP), Sodium Succinate, Adenosine Diphosphate (ADP), Apyrase, Phenylmethylsulfonyl Fluoride (PMSF), Digitonin and Coomassie brilliant Blue R were manufactured by Sigma Chemical Company (St. Louis, MO, USA). Reagents for SDS-PAGE and immunoblotting were purchased from BioRad (Richmond, CA, USA). All drugs were of analytical grade.

Mitochondria purification and incubation conditions

This study was carried out in strict accordance with the recommendations in the Guide for the Care and Use of Laboratory Animals of the National Institutes of Health. The rats were maintained in proper conditions in the animal facility of CEDIE and the experimental protocol was approved by Institutional Committee of Care and Use of Laboratory Animals of the Hospital Garrahan (CICUAL). Isolation of mitochondria was carried out as described by Rickwood et al. (1987), with some modifications. Male Wistar rats between 200 and 250 g, were starved overnight and the livers (~15–18 g) quickly removed, cooled at 4ºC and the blood was washed off. They were then cut into small pieces, and buffer was added (2 ml/g liver tissue: 20 mM HEPES, 70 mM sucrose, 220 mM manitol, 1 mM EDTA, pH 7.4) and homogenized in a tissue grinder with teflon pestle. All materials and buffers were sterile. The homogenate was centrifuged for 10 min at 600x*g*, and the supernatant centrifuged again for 15 min at 7000x*g* in a Sorvall RC2-B (DuPont Company, Biomedical Division Newtown, Connecticut, USA). The precipitated was diluted to half of the initial volume, centrifuged in the same conditions, and the new precipitated was treated as before. We measured the contamination in each mitochondrial fraction. The outer membrane had LDH (mU/mg proteins) 8.52 % and in inter-membrane space we found LDH contamination of 1.43 %. In mitoplasts we found a small amount of LDH (1.24 %) and our level of mitochondrial purification was 108 %.

The final precipitated was diluted in 20 mM HEPES, pH 7.4, 0.25 M mannitol, 5 mM PO_4K_2, 5 μM Cl_2Mg, 1 mM DTT, 50 μM Coenzyme A, 50 μM Cocarboxylase, 1 mg/ml bovine albumin fatty-acid free (buffer mitochondria), separated in batches and incubated at 25 °C with mild oxygenation for 15 min. After recovery, the mitochondrial experiments were conducted at 25 °C in batches, and a sample (250 μl) was obtained at each time between 0 and 300 s. as described in the figures. We named Control the tubes without

IDE because the addition of IDE was considered as Experimental. The experiments were calculated to contain in each tube: 1.2 μg/IDE, ~50,000 c/m ^{125}I-insulin + 1 ng of native insulin and ~1 mg of mitochondria. They were carried out in different experiments with the following drugs: 200 μM 2,4-dinitrophenol (DNP), 5 mM sodium succinate + 2 mM ADP, 1 mg/ml Bacitracin or 15 units of apyrase. Previous to addition of IDE and insulin, mitochondria were incubated with Bacitracin and DNP during 60 s at 25 °C, and with apyrase 15 min at 30 °C. The 250 μl were received in tubes with 1 mM NEM in buffer mitochondria without cofactors (NEM buffer) and placed in ice bath to stop the reaction. The tubes were centrifuged at 4 °C, during 7 min at 5,000 RPM in an Eppendorf micro-centrifuge and the pellets were suspended in 150 μl of 1 mM NEM buffer. Digitonin was added at a concentration of 1.2 %/mg mitochondria and the tubes were incubated at 2 °C during 15 min, suspended in three more volumes of NEM buffer, centrifuged at 13,000 RPM and mitoplasts (M) was separated from outer membrane + inter-membrane space (OM + IMS). Radioactivity was counted in supernatants and precipitates.

Confocal microscopy

The rats were fasted for 12 h, and mitochondria were isolated as described before. All mitochondria were incubated with 1 ng insulin/mg of mitochondria, without or with the addition of 1.7 μg IDE. Mitochondrial pellets were dehydrated after fixation by successive steps in increasing alcohol concentration, included in paraffin, cut in 3–4 μm, placed in Superfrost-Plus (+) slides (Corning Glass, One Riverfront Plaza Corning, NY, USA); the paraffin was taken away and washed. The pellets were covered with PBS, pH 7. After two washes in PBS, the slides were covered with 1/10,000 specific anti-porcine insulin antibody (SAI 15, guinea pig) or 1/750 specific monoclonal anti-IDE antibody (9B12, mouse), and incubated overnight at 4 °C in a damp chamber. Having been washed, the pellets were incubated with a specific second antibody: rabbit anti-guinea pig IgG-FITC (Zymed Lab. Carlton Court, San Francisco, CA, USA) or goat anti-mouse IgG-Cy3 (Zymed Lab. Carlton Court, San Francisco, CA, USA) during 1 h at room temperature. Then the pellets were washed twice with PBS and kept in a damp chamber. Confocal studies were made by means of an Olympus FV300 (Olympus Imaging America Inc., Corporate Parkway, Center Valley, PA, USA) with 3 lasers, Ar 488 nm; HeNe green 543 nm; HeNe red 633 nm; two immersion objective UplanApo (PlanApo 40x and PlanApo, 60x); scanners 3D (XYZ, vectorial-Z) with 0,025 μm increases in Z and zoom of 2.5x, 3x and 6x. Images were obtained with FluoView software version 3.3 and Kalman filtrate.

Enzyme purification

The purification procedure was similar to the one described before (Camberos et al. 2001) with some slight changes. IDE was extracted from the muscles and partially purified by multiple steps in DEAE-Sephadex A50. IDE was then adsorbed in a hydrophobic column, eluted in a gradient of ammonium sulfate and subjected to chromatography with FPLC (Pharmacia Diagnostics AB, Uppsala, Sweden) in a Mono Q column. This column was equilibrated with 20 mM Tris–HCl buffer, pH 7.4 and eluted with a lineal NaCl gradient from 0 to 500 mM in the same buffer. IDE obtained in these conditions was either used for studies or concentrated and purified further in Sephadex G200 superfine (50 ml column), equilibrated with 20 mM Tris-HCl pH, 7.4, 50 mM NaCl and 1 mM DTT. Fractions with degradation activity were stored at -70 °C and before its use we controlled the IDE activity in each fraction with the same degradation conditions. For different IDE extractions we compared both extractions with immunoblot and degradation in the same conditions.

All the above steps were performed at 4 °C and the protein concentration was assayed by absorbance at 280 nm in a spectrometer (Spectronic 3,000, array; Markham, Ontario, Canada) or by Bradford's methods. The samples of all purification steps were subjected to 7.5 % SDS-PAGE and stained with Coomassie Blue.

Degradation assay

Insulin degradation was incubated in 50 mM Tris-HCl buffer, pH 7.4 with 1 % bovine serum albumin (BSA), 10 mM $MgCl_2$, 2 mM $MnCl_2$ and 16–20 pM of ^{125}I-insulin (final incubation volume 100 μl). ^{125}I-porcine insulin was labeled with the Chloramine-T method and purified with preparative starch gel electrophoresis followed by Sephadex G50 Superfine chromatography (50 ml column) eluted with 20 mM HEPES, 7.4 pH and 0.01 % bovine albumin fatty-acid free. Insulin was predominantly labeled in tyrosine A-14 with a specific activity between 250 and 300 mCi/mg and a conserved biological activity (Cresto et al. 1981).

Degradation conditions were selected to preserve linearity during the incubation period. Degradation was stopped by the addition of trichloroacetic acid (TCA) 5 % of the final concentration, centrifuged for 15 min at 1000x*g* and pellets were separated from supernatants. Degradation was performed in duplicate or triplicate, and calculated as the increase in ^{125}I-insulin fragments (TCA soluble). Labeled insulin controls had more than 95 % of intact insulin; hence, experimental results were corrected for this value.

Insulin degradation in mitoplasts

After incubation with 1.2 μg/IDE, ~50,000 c/m ^{125}I-insulin + 1 ng of native insulin and ~1 mg of mitochondria, degradation in M or OM + IMS was measured by chromatography. Mitoplasts were incubated for 2 h at 4 °C with 2 % Triton X-100, centrifuged at 13,000 RPM, 4 °C in an Eppendorf microcentrifuge and the supernatant subject to chromatography in Sephadex G50 Superfine (25 ml column) eluted with 1 M acetic acid, 150 mM NaCl, 0.25 % bovine albumin. We precipitated and dissociated the first peak found in the chromatography with TCA 50 %, to analyze it by a new chromatography. Insulin and its degradation products were counted, characterized by its eluted position, TCA precipitation and immunoreactivity with anti-insulin antibody excess. Each peak area was calculated and expressed as the percentage of the total area. Radioactivity was counted in a gamma counter (Packard Instrument Company, Inc., Downers Grove, Illinois, USA).

Kinetics analysis of [insulin-IDE] association to mitoplasts

The association of [IDE-insulin] and [mitoplasts] was analyzed as a bimolecular reaction. Experimental studies were developed previously looking for enzyme interactions, but they were not consistent. Increments of insulin mass showed that the interaction [IDE-insulin] and [mitoplasts] could be described as a bimolecular reaction following a second order reaction; which is dependent of time and the mass of reactants and both reactants can be modified independently one of the other. In this conditions the constant k can be calculated with the equation $t/q_t = 1/s + 1/q_c$. t as a "pseudo 2nd order reaction" as proposed by Ho and McKay (Ho & McKay 1999); where "q_t" is the concentration of "a" at the experimental time "t" and "q_c" is the value of "a" in equilibrium. A plot of "t/q_t vs. t" will give a straight line and the slope will be equal to "k".

Mitochondrial cross-linking

Between 1.5 and 2.5 mg of mitochondria were incubated for 60 s at 25 °C in 125 μl of buffer mitochondria with ^{125}I-insulin (~6×10^5 c/m) alone, or with the addition of 1.2 μg/tube of IDE, or the same plus 10 μg/tube of native insulin. The reaction was stopped with 1 mM NEM buffer and cooling the tubes in ice bath. Then, they were centrifuged and the pellet suspended in 150 μl of the aforementioned buffer. Digitonin (1.2 %/mg mitochondria) was added to mitochondria and incubated during 15 min at 2 °C. The mitochondrial suspension was centrifuged at 5,000 RPM and the pellet was diluted in 50 mM phosphate buffer, 100 mM NaCl, pH 7.4 and incubated for other 30 min at 2 °C with 9 μl of disuccinimidyl suberate (8.25 mM in DMSO; the final concentration being 0.46 mM). After incubation, 450 μl of buffer mitochondria was added and centrifuged at 13,000 RPM to obtain M and OM + IMS. The cross-linking was made after digitonin treatment because this sequence ensures that it was performed in OM + IMS and M. Mitoplasts were diluted in 100 μl of buffer mitochondria and 33 μl of concentrated sample buffer was added to each experiment and heated during 3 min at 100 °C. Forty five μl by line of OM + IMS and mitoplasts were subjected to electrophoresis in 7.5 % SDS-PAGE. Proteins were higher in mitoplasts than OM + IMS because it was diluted 4 times. Some gels were stained and dried, but other gels were transferred to nitrocellulose for immunoblot studies to detect insulin, IDE or TIM23. Autoradiography was made in gels and immunoblots; densitometer studies were performed with ScnImage software (based on NIH-Image on the Macintosh platform).

Immunoprecipitation of IDE from mitoplasts

Mitochondria were incubated at 25 °C during 300 s with 1 ng/tube of insulin, alone or with the addition of 1.7 μg/tube of IDE, or IDE + ATP (0.5, 2.5, 10 mM/tube). Mitochondrial incubation was stopped by cooling the tubes in ice bath with immediate addition of 1 mM NEM (final concentration). Mitochondria were treated with digitonin to isolate mitoplasts and they were quickly frozen in liquid nitrogen and thawed. This procedure was repeated 3 times and mitoplasts were sonicated 5 times during 5 s at 100 watts in ice bath (Ultrasonics sonicator, Branson Ultrasonic Corporation, Danbury, USA), centrifuged and the supernatants were incubated overnight at 4 °C with 20 μg/tube of anti-IDE antibody 9B12 (kindly provided by Richard A. Roth, Stanford University, Stanford, CA). These tubes were incubated other 4 h at 4 °C with 300 μg of IgG-agarose goat anti-mouse. The immunoprecipitated enzyme was centrifuged at 13,000 RPM, 10 min, 4 °C. The pellets were washed, centrifuged again, suspended in 60 μl of buffer, and 20 μl of concentrated sample buffer were added. The pellets were boiled and centrifuged again before the electrophoresis in 10 % polyacrylamide gel slabs.

SDS-PAGE and Immunoblot

Proteins (10 to 45 μg by line, depending on the study) were subjected to SDS-PAGE electrophoresis in 7.5 % gel slabs and stained with Coomassie Blue or transferring for immunoblot. IDE was detected in immunoblot with 1/500 immunopurified carboxiterminal specific rabbit anti-IDE p15 (Camberos et al. 2001) or 1/750 monoclonal anti-IDE antibody 9B12. TIM-23

was detected with a specific goat antibody with 1/100 dilution (Santa Cruz Biotechnology, Dallas, Texas, USA). Prior to color development, monoclonal anti-IDE antibody was incubated for 1 h at room temperature with 1/250 dilution rabbit anti-mouse IgG or TIM-23 with 1/250 dilution of rabbit anti-goat IgG. Rabbit insulin antibody (kindly provided by Dr. Juan C. Basabe) was used in some immunoblots to confirm the insulin position.

When the study to detect insulin was performed in immunoprecipitated IDE, the SDS-PAGE electrophoresis was in 10 % polyacrylamide slabs. The immunoblot was incubated overnight at 4 °C with 1/1,000 dilution of specific insulin guinea pig antibody (SAI 4) followed by 2 h incubation with 50 μg/ml of rabbit anti-guinea pig. The immunoblots were stained with alkaline phosphatase-conjugated goat anti-rabbit IgG according to the manufacturer's protocols. Pre-staining standards were used as molecular weight controls.

Statistic Some experiments were expressed as percentage changes of its own basal condition to allow comparisons between control and IDE, but the statistical significance was always calculated with the absolute values. The significance between groups (<0.05) was determined with GraphPad Prism 4 (GraphPad Software for Windows, San Diego, Ca, USA) and they were calculated as unpaired *t* test.

Results

Electron microscopy showed preservation of organelles ultrastructure (Fig.S1) and it can be observed membranes but there was a little peroxisomal contamination and we can not found contaminate lysosomes. The studies demonstrated low concentration of lactic dehydrogenase and catalase, suggesting low cytosolic and peroxisomal contamination. We measured the contamination in each mitochondrial fraction. The outer membrane has LDH (mU/mg proteins) 8.52 % and in intermembrane space we found 1.43 % contamination. Total LDH contamination was 11.48 % and the outer membrane was the highest value. Our level of mitochondrial purification was 108 % (mg mitocondrial proteins/grams wet weight liver).

To know if insulin could be degraded by mitochondrial proteases released during incubation studies, the mitochondrial wash were incubated with ^{125}I-insulin at 25 °C during 300 s. The results demonstrated that insulin degradation was minimal (pg/min/mg; Control: 10.2; IDE: 12.6) and they were dependent on mitochondrial proteases because insulin degradation by isolated IDE was absent at this temperature (Fig. S2). Insulin and mitochondria can be considered as constant during incubation and experimental changes can not be ascribed to associated degradation because the results showed mitochondrial and insulin integrity.

Mitochondria incubated at 25 °C with increasing insulin concentration during 60 or 120 s did not show an increase in insulin accumulation in OM + IMS or M (not shown), but increments of IDE to isolated mitochondria induced an insulin increase in M over the basal value which was observed at two different times (Fig. 1). There were no modifications in OM + IMS (not shown) and these results demonstrated that increments of IDE increased insulin in M. To analyze these results we studied the insulin accumulation in OM + IMS and M at different times without or with IDE. The enzyme induced a statistical increment of insulin in M, and this behavior was not observed in OM + IMS although they had higher insulin values than in M (Fig. 2a-b). In order to know how IDE facilitates the insulin accumulation in M, we studied other drugs. Insulin and Bacitracin compete to be bound by IDE, and this competition was demonstrated in Fig. 2c-d, where insulin was displaced by Bacitracin in OM + IMS, the same as Control or IDE. Bacitracin pre-incubation and competition with endogenous IDE could explain the inhibition of insulin accumulation in Control. It is known that mitochondrial protein incorporation depends on the transport system from OM to Mx. It requires energy to reach the mitoplasts and it is known that IDE with long presequence is transported to mitochondrial matrix. The addition of uncouples of oxidative phosphorylation in mitochondria like DNP would impede or slow down the insulin transfer if the enzyme would be an insulin carrier. DNP was ineffective to modify insulin accumulation in OM + IMS, but insulin in M was decreased to basal levels (Fig. 2f). This last figure appears to have only 3 experiments because IDE + DNP are not visible due to Control + DNP have similar values.

We analyze the kinetics of insulin association to mitoplasts in these last two experiments because insulin, IDE and M concentration had remained without modifications in our incubation conditions. We could therefore consider [IDE-Insulin] and [Mitoplasts] as molecular reactants in a bimolecular reaction. If the velocity of the reaction was sensitive to the concentrations of both reacting species, the reaction would follow a second order kinetic (Fig. S3). Both molecular species [IDE-Insulin] and [Mitoplast] participate and could be modified independently. The study showed (Fig. 3a-b) that constant k (liter.mol^{-1} s^{-1}) was **Bacitracin (A)**: Control 7×10^{10}; IDE 4×10^{10}; Bacitracin (Control) 8×10^{10}; IDE + Bacitracin 5×10^{10}, and with **DNP (B)**: Control 7×10^{10}; IDE 4×10^{10}; DNP (Control) 6×10^{10}; IDE + DNP 7×10^{10}. IDE increased the velocity of insulin accumulation in mitoplast, and the addition of Bacitracin or DNP decreased this velocity. The mitochondrial mechanism of action of both drugs differed, one by insulin competition with IDE and the other decreasing the ATP concentration in mitoplasts, however the results were similar.

We studied other inhibitors and substrates, such as 5 mM sodium succinate + 2 mM ADP or 15 U of apyrase (Fig. S4).

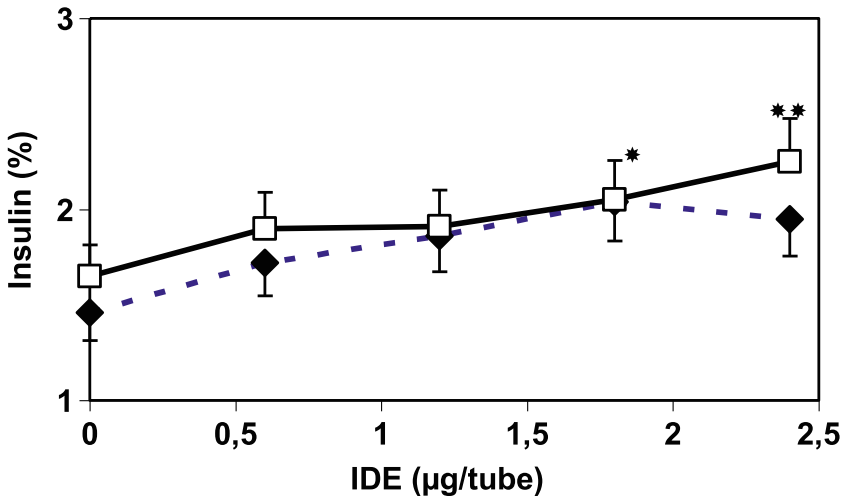

Fig. 1 Insulin accumulation in mitoplasts. ♦ - Incubation time 60 s. □ - Incubation time 120 s. ^{125}I-insulin + 1 ng insulin were incubated at 25 °C with increased concentrations of IDE.Time 60 s: IDE "0" (no IDE addition) vs IDE 1.8 µg/tube (n: 4): $p<0.02$*. Time 120 s: IDE "0" (no IDE addition" vs IDE 2.4 µg/tube (n: 4): $p<0.05$**. Insulin accumulation in mitoplast was dependent on IDE concentration

Apyrase was pre-incubated 15 min at 30 °C and did not modify the insulin accumulation in OM + IMS but in mitoplasts diminished the increments produced by IDE. This decrease in M did not reach to be significant, but indicates that a decrease of ATP can modify the increment induced by IDE. We also studied succinate + ADP looking for an induction of metabolic response, but the experimental conditions were not sufficient to induce insulin changes.

We used gel filtration chromatography in solubilized M to determine the amount of free insulin. The chromatography showed three radioactive peaks at all times, similar in Control or IDE (Fig. 4). The first peak was the v/v (size-exclusion in gel-filtration chromatography or void volume) the second peak was in the position of free insulin, and the third peak, always small, in the position of degraded insulin. The mitoplasts Control only showed a defined first peak at 300 s of incubation with a small second peak. IDE showed a big first peak at basal time with a small second peak of free insulin, but at 300 s the first peak decreased and the second peak increased (61 %, Fig. 4). Insulin distribution in the last chromatography was verified with insulin antibody excess (dilution 1/20,000), which demonstrated that the second peak was free insulin. That is, IDE changes insulin distribution in mitoplasts during incubation and the first peak became free insulin after 300 s.

The chromatography of solubilized mitoplasts showed the first peak in v/v position (Sephadex G50 superfine). This could be the expression of different, isolated proteins of high molecular weight or interacting, associated proteins showing a molecular weight higher than 100 kDa. In order to understand how the first radioactive peak was formed we dissociated this protein complex using TCA precipitation at 50 % and we identified insulin by its chromatographic position (Fig. 5) and IDE in immunoblot by the specific 9B12 antibody (Fig. 5, Inset). The peaks distribution were in the first chromatography: 1st Peak: 69 %, 2nd Peak: 31 %; second chromatography after dissociation: 1st Peak: 54 %, 2nd Peak 47 %. The amount of degraded insulin was similar in both cases, thus in our study conditions the first peak formation in mitoplasts was IDE, none degraded insulin, and other unknown proteins.

In order to analyze this point, we made a mitochondrial cross-linking with labeled insulin (Fig. 6). Gel autoradiography of insulin cross-linking showed a dark spot in a position unrelated to insulin molecular weight (Fig. 6,1a; 136 kDa and 180 kDa), which was increased by IDE and was inhibited by unlabeled insulin (Fig. 6,1a line 3). These radioactive spots were not visible in OM + IMS (lines 4, 5, 6), but free insulin radioactivity was visible at the bottom, and a subtle image was present in line 5 (Fig. 6,1a). These results suggested an [IDE-insulin] complex because the enzyme addition increased radioactivity in line 2 and also increased the radioactive spot at 180 kDa which coincided with a higher MW of IDE in immunoblot (Fig. 6,1a lines 1, 2, 3 and immunoblot B). The protein concentration of OM + IMS was lower than in M, but this difference did not explain the results because the dilution was not sufficient to impede a visible image after long autoradiography exposure. Three similar experiments showed the same and suggested that cross-linking was ineffective in OM + IMS or that the traffic in this fraction was faster and escaped to cross-link procedure. Other cross-linking studies were performed with TIM23 and IDE antibodies (Fig. 6.2). We found with TIM23 antibody a 160 kDa band in isolated inner membrane used as TIM23 control (Fig. 6.2, IM). Three bands of TIM23 were coincident with IDE (150, 136, 125 kDa) and densitometry studies showed with IDE antibody that IDE addition produce a statistical increment of IDE bands (Fig. 6.2, IDE Ab, a-b). TIM23 antibody showed a statistical increment with IDE in 150 and 136 kDa bands, but was not significant in 125 kDa (Fig. 6.2, TIM23 Ab, a-b). Autoradiography of TIM23 immunoblot with IDE addition (Fig. 6.2a) showed

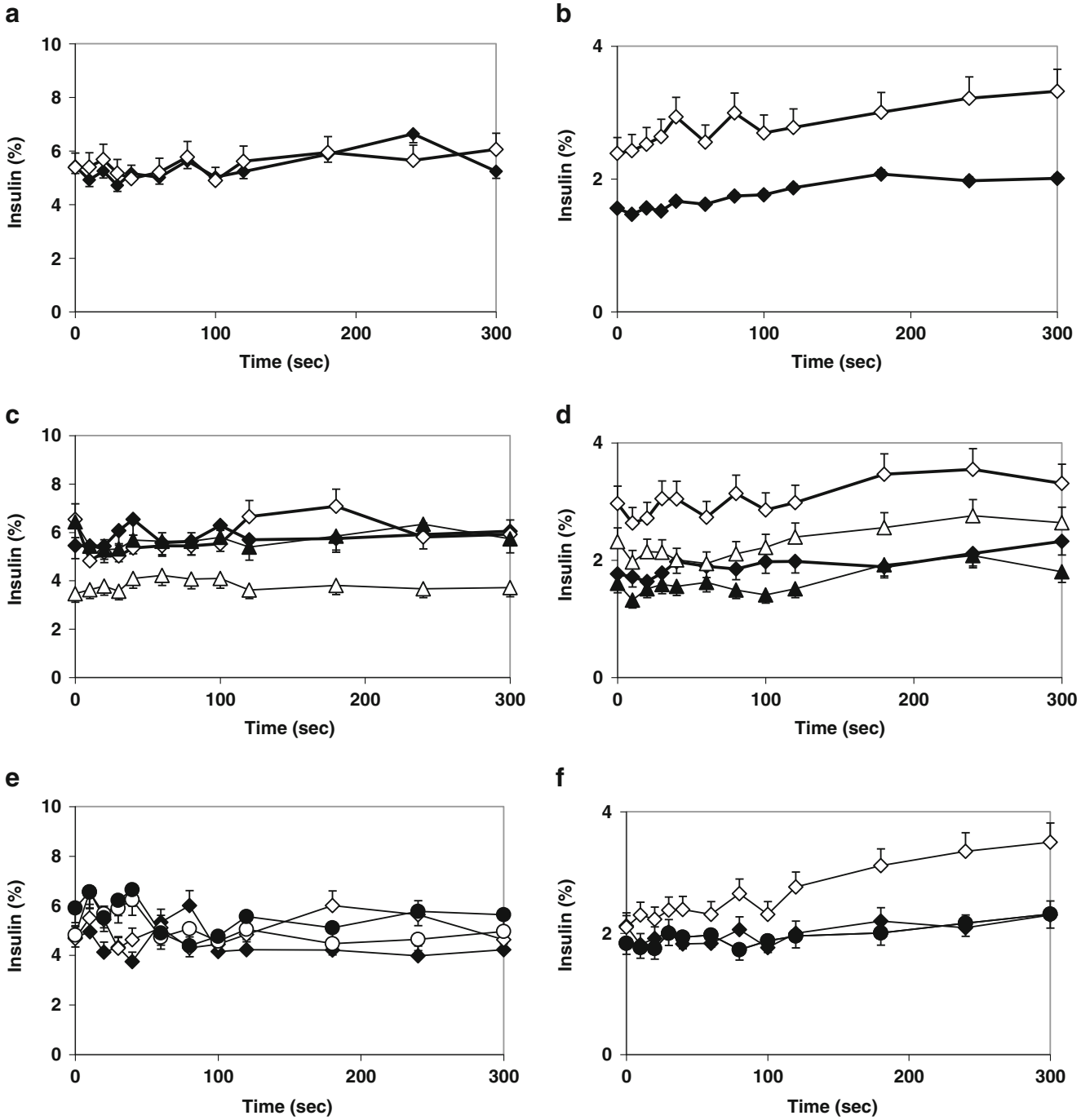

Fig. 2 Insulin accumulation in outer membrane + intermembrane space and mitoplasts. **a (OM + IMS):** Control (♦), IDE (◇),(n: 9); **b (M):** Control (♦), IDE (◇) (n: 9); **c (OM + IMS):** Control (♦), IDE (◇), Control + Bacitracin (▲), IDE + Bacitracin (△) (n: 7). **d (M):** Control (♦), IDE (◇), Control + Bacitracin (▲), IDE + Bacitracin (△)(n: 7); **e (OM + IMS):** Control (♦), IDE (◇), Control + DNP (●), IDE + DNP (○) (n: 4); **f (M):** Control (♦), IDE (◇), Control + DNP (●), IDE + DNP (○) (n: 4). IDE + DNP is not visible because Control + DNP have similar values. **Statistic. a (OM + IMS)** - There were not statistical differences in Control or IDE. **b (M) -** Control vs IDE (n: 9): all times were statistically significant ($p<0.05$ to $p<0.005$). Control "0" vs 180 or 300 s. were statistically significant. **c (OM + IMS) -** IDE (n: 9) vs IDE + Bacitracin (n: 3) "0" vs 120 or 240 s. were statistically significant. **d (M) -** Control vs Control + Bacitracin (n: 6): times 100, 120, 300 s. were statistically significant. IDE vs IDE + Bacitracin (n: 3): times 40, 100 s. were statistically significant. **e (OM + IMS) -** There was not statistical differences. **f (M) -**. IDE vs IDE + DNP (n: 3): times 40, 60, 80, 180 s. were statistically significant. The addition of IDE did not induce changes in OM + IMS, but increased the insulin accumulation in M. Bacitracin decreased the insulin accumulation by IDE in OM + IMS and M, and also decreased the insulin accumulated in Control. Addition of DNP did not modify insulin in OM + IMS but decreased the insulin accumulated by IDE in M

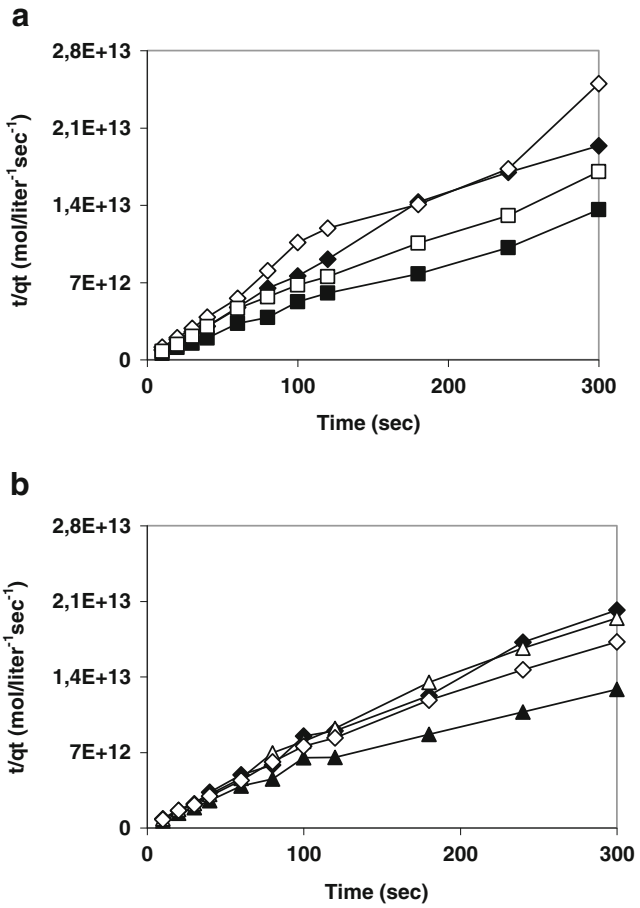

Fig. 3 Kinetic of [Insulin-IDE] and [Mitoplasts]. a - Bacitracin: Control (♦); IDE (■); Control + Bacitracin (◇); IDE + Bacitracin (□). **b - DNP:** Control(●); IDE (▲); Control + DNP (○); IDE + DNP (△). **The constant *k* is expressed in liter.mol^{-1}s^{-1} Bacitracin -** Control: 7×10^{10}; IDE: 4×10^{10}; Control + Bacitracin: 8×10^{10}; IDE + Bacitracin: 5×10^{10}. **DNP-** Control: 7×10^{10}; IDE: 4×10^{10}; Control + DNP: 6×10^{10}; IDE + DNP: 7×10^{10}. Modification of insulin incorporation to mitoplasts can be obtained by changes in either one of molecular reactants [IDE-Insulin] or [Mitoplasts] as described in the 2nd order reaction. The [IDE-Insulin] complex behaves as a molecular unit

radioactivity in 136 and 115 kDa bands, the last in position of IDE, and 3 other of 83, 76 and 56 kDa that could belong to degraded IDE.

To confirm the insulin position during cross-linking we studied immunoblots with IDE and insulin antibodies. We found bands at 150 and 136 kDa recognized by both antibodies (Fig. S.5a - IDE antibody and Insulin antibody) suggesting that in mitoplasts, insulin and IDE were together. The autoradiography confirmed that IDE bands of these immunoblots (Fig. S.5b) were coincident with the spots of radioactive insulin of Fig. 6,1a, showing the same low radioactivity observed in OM + IMS in the gel autoradiography Interestingly, the 136 kDa band was previously identified by its radioactivity in all the studies (Fig. 6.1; 6.2).

We immunoprecipitate IDE from matrix of isolated mitoplasts after mitochondrial incubation to determine if insulin bound to IDE was degraded at 25 °C. We observed previously that 0.5 mM ATP increased IDE insulin binding (Camberos et al. 2007) and we intend to observe if mitoplasts IDE would have the same behavior. We found that IDE incremented insulin accumulation and ATP at low concentration (0.5 mM ATP) increased the hormone accumulation in OM + IM: (% of insulin in OM + IMS, Media ± SEM, n: 3) - Control (no IDE): 4.08±0.18; IDE: 5.52±0.13; IDE+0.5 mM ATP: 7.17±0.65; IDE+2.5 mM ATP: 5.11±0.06; IDE+ 10 mM ATP: 5.41±0.24.

The same material was used for IDE immunoblot with the aggregated of line 1 (insulin control, 10 μg of native insulin) (Fig. 6.3). We observed intact insulin at 5.8 kDa in all lines. Densitometry showed that lines 2 and 3 did not show differences between them, the same that lines 4 and 6. Lines 2 and 3 were statistically higher than lines 4 or 6, and the same lines 4 and 6 were higher than line 5. ATP at low concentration (0.5 and 2.5 mM) decreased slightly the free insulin released from IDE, but insulin decreased clearly in 10 mM ATP. The study demonstrated in mitochondrial matrix, that insulin bound to IDE at 25 °C can be released as none degraded insulin.

Confocal studies Figure 7 showed mitochondria incubated with 1 ng/tube of insulin and 1.7 μg/tube of IDE. IDE antibody (Fig. 7a, red) showed mitochondria with many shapes and sizes that probably corresponded at more than one plane of section. The same studies with porcine insulin antibody (Fig. 7b, green) showed less labeled mitochondria than the figure A, and when both antibodies were superimposed (Fig. 7c, yellow, merge) the figure showed yellow mitochondria which were coincident with the number and position of green in the figure B. In this condition about 100 % of green mitochondria became yellow (merge) when IDE was added. When IDE was not added (rats with endogenous IDE concentration) only 58 % of green mitochondria became yellow (merge, not shown). Therefore rat IDE at its basal mitochondrial concentration was not sufficient to bound 1 ng of added insulin. To know how [Insulin-IDE] complex were distributed inside the rat mitochondria we isolated 1 mitochondrion (Fig. 7d) and we observed that green image was slightly large in comparison with red image which appeared to be more compact. We cut the mitochondrion 16 times with the laser with a wide of 0.025 μm section. Looking at the sequential sections, it was observed that the stained insulin (green) appears before the stained IDE (red), and a magnified image of this mitochondrion (Fig. 7e, section 7; Z position z: 1.75 μm dept) showed green at one side, red in the other side and yellow in the middle, suggesting that [Insulin-IDE] complex arrived together to mitochondria and then were dissociated.

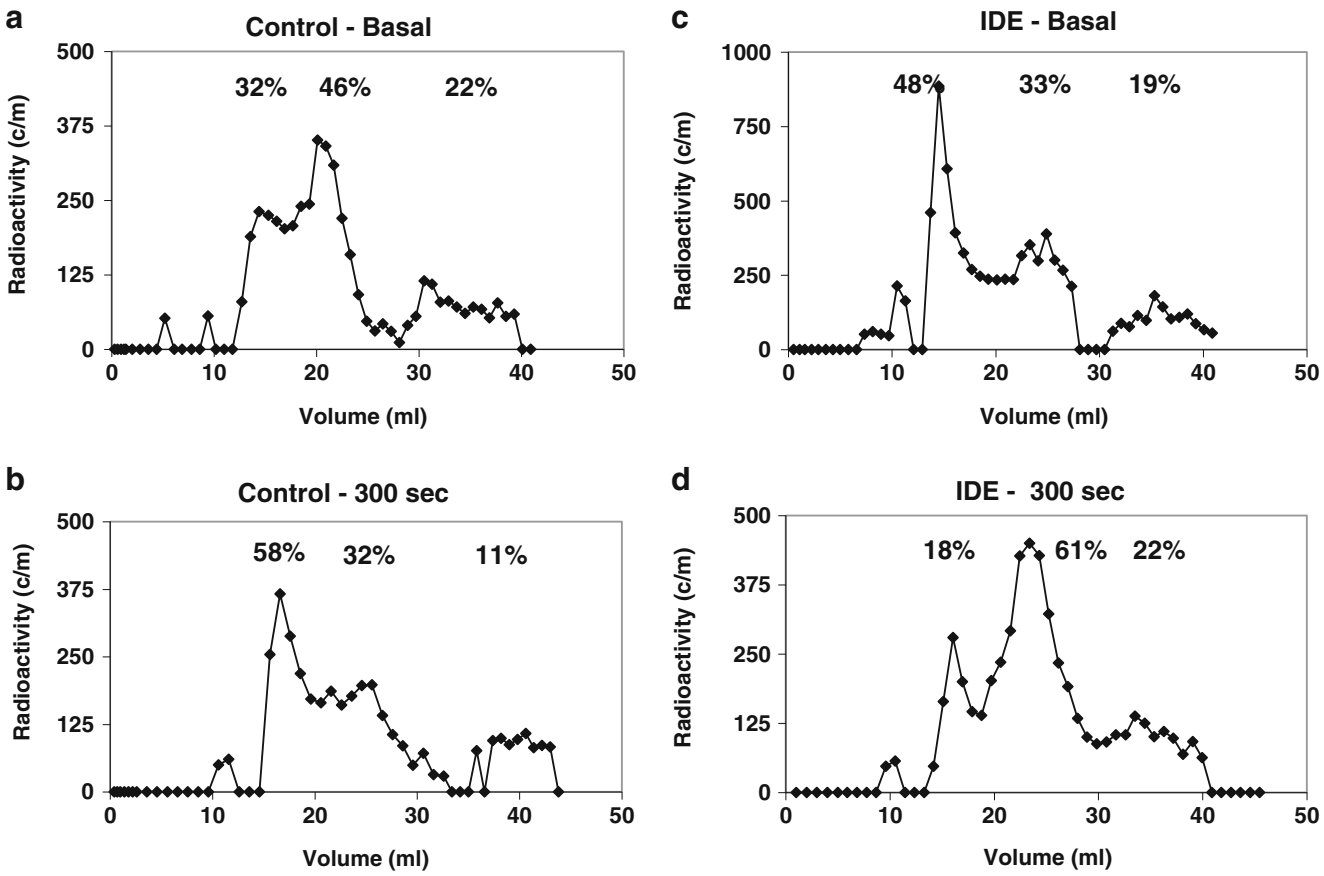

Fig. 4 Chromatographic profiles of mitoplasts. **a -** Control insulin at basal (basal mean 3-4 s. of time expended to withdraw the sample); **b -** Control insulin at time 300 s; **c -** Insulin + IDE at basal; **d -** Insulin + IDE at time 300 s. Mitoplasts of three individual experiments by duplicates were joined at each time and treated with 2 % Triton X-100 during 2 hs, centrifuged and the supernatant were subject to chromatography in Sephadex G50 superfine. The results with anti-insulin antibody excess (1/20,000) in the chromatography of Fig. 4, **d** showed: 1st peak position (size-exclusion in gel-filtration chromatography or void volume): 4.75± 1.41 (n: 6); 2nd peak (free insulin) 82.73±5.11 (n: 14); 3rd peak (degraded insulin) 1.13±0.93 (n: 5). Radioactive areas are expressed as % values

Discussion

IDE was extracted from rat muscle because the extracted enzyme kept the described relation between cytosol, peroxisome and mitochondria (Authier et al. 1995; Leissring et al. 2004). IDE with mitochondrial signal (long precursor) has been estimated nearly 30 % of total IDE (Leissring et al. 2004; Im et al. 2007) and we take this concept into account when we evaluate the experimental results.

Insulin accumulation in mitoplasts appears to be dependent on IDE concentration because increments of insulin without IDE did not increase the insulin concentration. The accumulation of insulin in mitoplasts did not correlate with the amount of IDE added since only a third of IDE was directed to mitoplasts. When the amount of IDE added was small, endogenous IDE increased the insulin accumulated in M as observed in Fig. 1 and could explain the absence of correlation. The time dependent insulin accumulation in Fig. 2 could suggest that added IDE continues its activity increasing this insulin accumulation. These results were more visible due to absence of degradation at 25 °C.

Insulin found in OM + IMS was always higher than M but this insulin concentration was not modified by IDE or drugs addition. Only Bacitracin, as insulin competitor with IDE, decreased the insulin accumulation in OM + IMS. The same happens in Controls (mitoplasts without IDE) demonstrating it was specific insulin association between insulin and endogenous rat IDE. Otherwise, as expected in non specific insulin binding, Bacitracin should not decrease Control without IDE. DNP an uncoupling agent that function still at low temperature (Ezaki et al. 1982) had limited functions in OM + IMS but it could decrease the driving proton input in mitoplasts and IDE transfer, also decreasing insulin radioactive counts which was what we measured.

We studied the kinetic interaction between [IDE-Insulin] and [Mitoplasts] at 25 °C because at this temperature the insulin degradation was negligible, and the reactants could be considered stable. The objective was to describe IDE + insulin as a complex association and participant with

mitoplasts in a bimolecular reaction. In general, if the velocity of the reaction is sensitive to the concentrations of both reacting species, the reaction followed a second order kinetic $da/dt = -kab$, but if one of the reactants remains constant during the time "*t*" in the reaction, a common solution is to calculate the constant as *pseudo first order reaction*. Another possibility is to calculate the constant as *pseudo second order reaction* as described by Ho and McKay (Ho & McKay 1999) whose final equation is $t/q_t = 1/s + 1/q_c.t$ (where "q_t" is the concentration of "*a*" at the experimental time "*t*" and "q_c" is the value of "*a*" in equilibrium). A plot of "t/q_t vs. *t*" will give a straight line and the slope will be equal to "*k*".

Bacitracin and DNP can modify each of the reactants independently, as described in a second order reaction. In this study the experiments were performed with a low insulin concentration (1 ng/mg tube of mitochondria) accepted as the normal insulin concentration in the liver. The constant showed that Bacitracin and DNP decreased the velocity of insulin transfer from OM + IMS to M; Bacitracin acting on the insulin binding and modifying the complex association between [IDE-Insulin], and DNP changing the mitocondrial input to transfer proteins. As showed by other authors Bacitracin, a low affinity IDE inhibitor at the concentration of 1 mg/ml (700 μM) inhibits 70 % of IDE (Im et al. 2007). Moreover, the concentration used with DNP (200 μM) do not alter either the mitochondrial metabolism or cell viability but it was sufficient to decrease, still at this low temperature, the ATP accumulated in mitochondria (Ezaki et al. 1982; Mylotte et al. 2008). The study showed [IDE-Insulin] as a molecular unit because we only measured the radioactivity and there was a change by insulin competition or modification of ATP levels, suggesting that IDE in these conditions is "similar to" or "functions as" an insulin carrier. In concordance with these results, IDE facilitates the incorporation of steroid receptors in nucleus after steroid stimulation but loosing its degradation activity in the organelle (Udrisar et al. 2005).

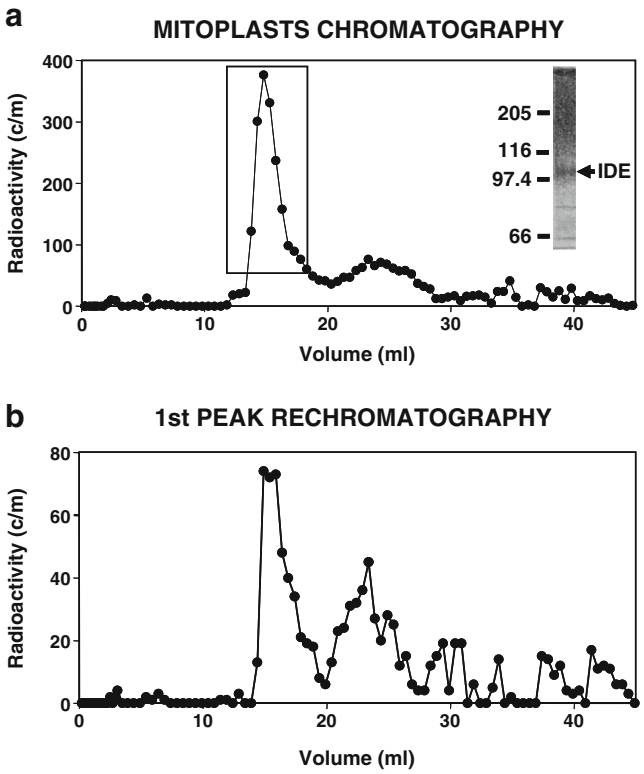

Fig. 5 First peak chromatography of solubilized mitoplasts. Mitochondria were incubated with 1.2 μg of IDE + insulin during 60 s. at 25 °C and treated as explained in material and methods. The first peak chromatography was isolated, precipitated with TCA 50 %, suspended in elution buffer and it was subject to a new chromatography (n: 2). **a**: mitoplasts chromatography. 1st Peak: 69 %, 2nd Peak: 31 %. **b**: first peak rechromatography. 1st Peak: 54 %, 2nd Peak 47 %. **Inset.** The first peak chromatography was lyophilized, diluted in 1.5 ml of water, centrifuged, concentrated in Centricon-100 Blue and subject to electrophoresis in SDS-PAGE followed by immunoblot. The specific 9B12 IDE antibody was used for IDE detection. The inset showed 110 kDa IDE with 75 and 66 kDa fractions of IDE. The first peak rechromatography (after chaotropic dissociation with 50 % TCA) showed a peak of free insulin without increment of degraded insulin in comparison with the first chromatography. The result suggests that the first peak was formed by a complex of [free insulin-IDE] associated to other proteins

Fig. 6 Immunoblot and autoradiography studies 6.1a - Autoradiography of gel (mitochondrial cross-linking, n: 3). Forty μl of sample were applied by line. Line 1: M + ^{125}I-insulin; line 2: M + ^{125}I-insulin + IDE; line 3: M + ^{125}I-insulin + IDE+10 μg native insulin; line 4: OM + IMS + ^{125}I-insulin; line 5: OM + IMS + ^{125}I-insulin + IDE; line 6: OM + IMS + ^{125}I-insulin + IDE+10 μg native insulin. Densitometry: line 1 (180 kDa): 100 %; line 2: 155 % ($p<0.0005$); line 3, 4, 5, 6: not visible. line 1 (136 kDa): 100 %; line 2: 115 % ($p<0.0005$); line 3: 13 % ($p<0.0005$); lines 4, 5, 6: not visible. MW markers are on the left. 6.1B - IDE immunoblot. The position of IDE is showed at 110 and 180 kDa. 6.2 - TIM23 and IDE immunoblots (mitochondrial cross-linking, n: 3). 6.2 TIM23 antibody. a: ^{125}I-insulin + mitoplasts. b: ^{125}I-insulin + IDE + mitoplasts. IM (inner membrane) showed a line at 160 kDa. Line markers indicate the position of 150, 136 and 125 kDa bands. 6.2 IDE antibody. a: ^{125}I-insulin + mitoplasts. b:^{125}I-insulin + IDE + mitoplasts. Line markers indicate the position of 150, 136, 125 kDa bands. IDE position was 117 kDa. Densitometry of TIM23 (no IDE vs. IDE): 150 kDa, $p<0.0003$; 136 kDa, $p<0.03$; 125 kDa, not significant. Densitometry of IDE (no IDE vs. IDE): all IDE bands are higher, $p<0.01$ to $p<0.0001$. 6.2A - Autoradiography of immunoblot TIM23: The autoradiography belong to TIM23 immunoblot with IDE addition (b). It showed 5 radioactive bands at 136, 112, 83, 76 and 56 kDa. The 136 kDa band was at the same position described in 6.1A. The 115 kDa band belongs to IDE (recognized by IDE antibody in immunoblot). 6.3 - Insulin immunoblot (IDE immunoprecipitated, n: 2).Line 1 - Insulin standard; line 2- Mx (alone); line 3 - Mx + IDE; line 4 - Mx + IDE + 0.5 mM ATP; line 5 - Mx + IDE + 10 mM ATP; line 6 - Mx + IDE + 2.5 mM ATP. Densitometry of insulin: line 2 vs. line 3: ns; line 4 vs. line 6: ns. Lines 2 and 3 vs. lines 4 and 6: $p<0.0001$. All lines vs. line 5: $p<0.0001$. Mitochondria were incubated at 25 °C with 1 ng/tube of insulin, insulin + IDE and insulin + IDE + ATP. IDE from sonicated mitoplasts was immunoprecipitated with the specific antibody 9B12 as described in Methods, and this IDE immunoprecipitated was analyzed in 10 % poliacrylamide gel slab and transfer for immunoblot. A specific insulin antibody (SAI 4) recognized the free insulin released from IDE immunoprecipitated

6.1 AUTORADIOGRAPHY OF GEL

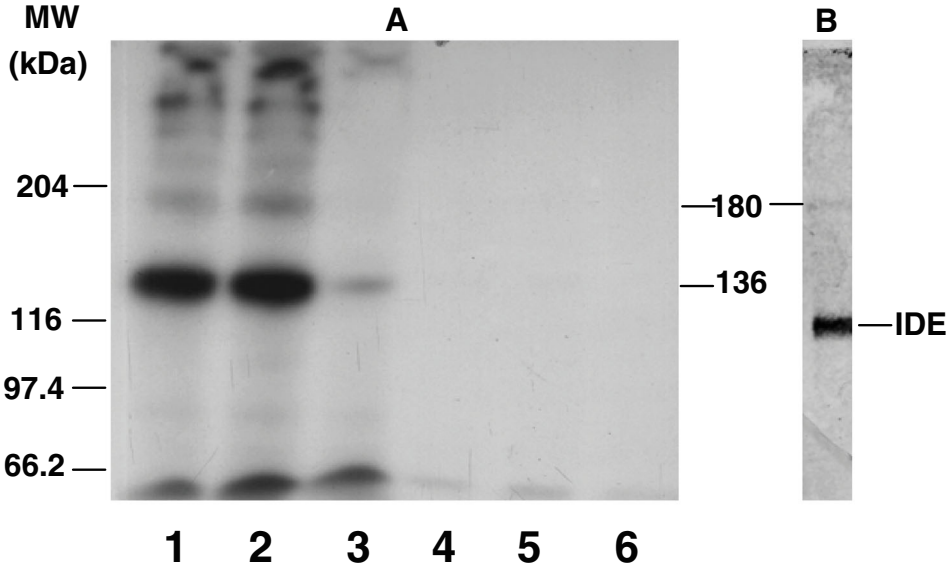

6.2 IMMUNOBLOT

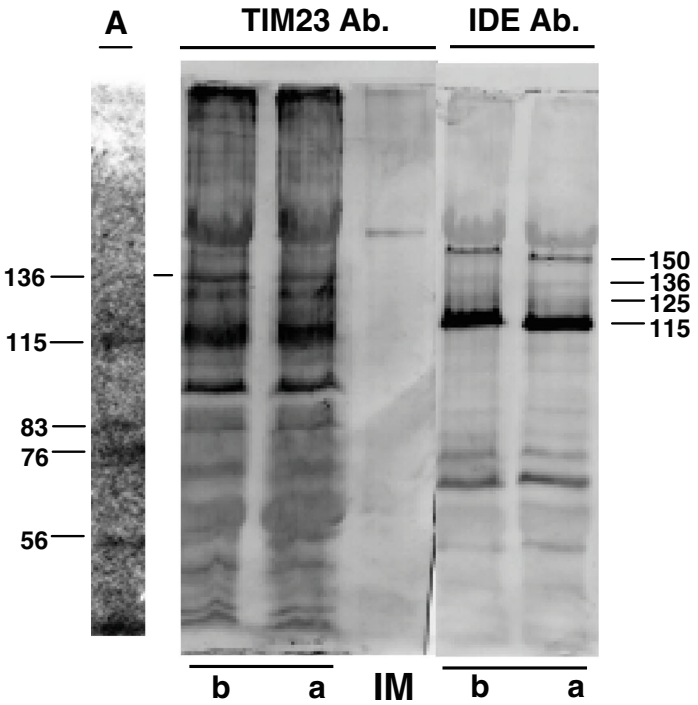

DENSITOMETRY (TIM23, IDE)

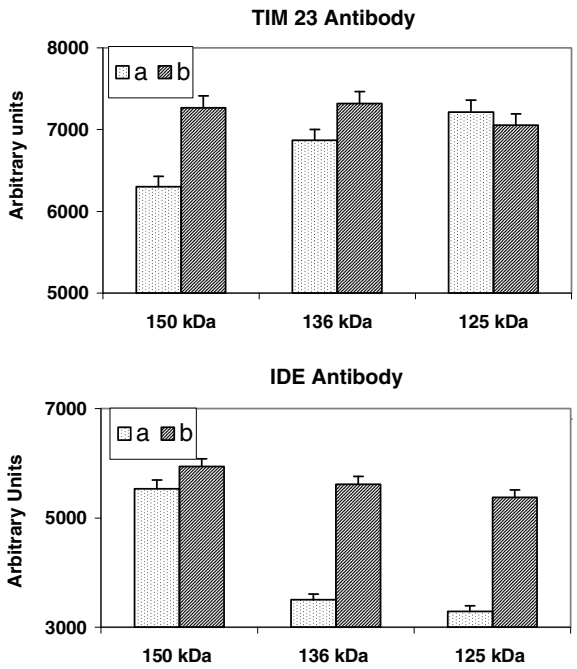

6.3 INSULIN IMMUNOBLOT
(IDE immunoprecipitated from Mx)

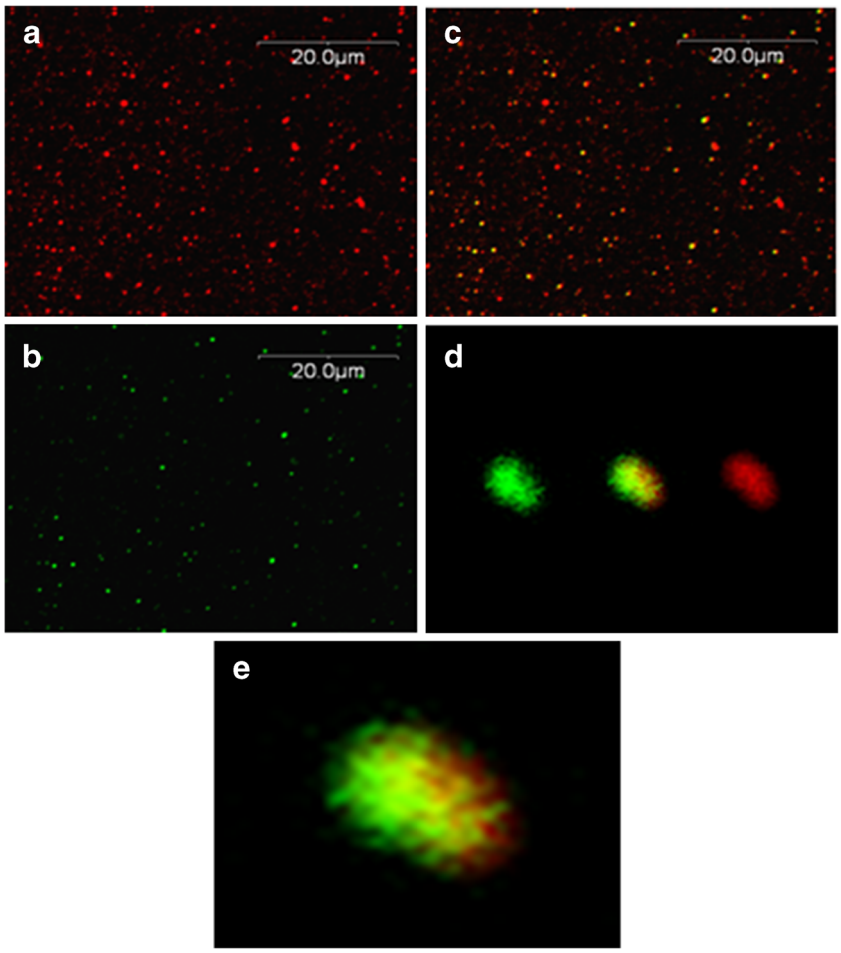

Fig. 7 Confocal studies. The study was performed as described in material and methods. Amplification 60x, zoom 6x. **a**: red, IDE antibody; **b**: green, porcine insulin antibody; **c**: yellow, merge. Bars=20,0 µm. **d**, it shows one mitochondrion (left) with insulin antibody, the same mitochondrion (right) with IDE antibody and in the middle both antibodies superimposed (yellow, merge). **e**: it shows the distribution of IDE and insulin in the same mitochondrion, cut with the laser: from origin 7th section [Z, vectorial z 1.75 µm]. The objective was 60x, zoom 6x; computer magnification 12 times. Effective increment 43200x

We observed with chromatography insulin increments in the second peak (free insulin) of mitoplasts. It could be either free insulin accumulated and released or insulin dissociated during chromatography, but the time required for this increment suggested the hormone was actively accumulated into the mitoplasts. We could hypothesize that insulin addition, such as addition of other hormones, increases IDE in mitochondrial matrix with insulin accumulation (Cesar Vieira et al. 2011).

From the three main peaks observed in mitoplasts chromatography, the first peak was formed immediately after IDE addition, suggesting the [IDE-Insulin] binding as the first step in insulin transfer. The study of this first peak in mitoplasts showed the interaction of [IDE-free insulin] without degradation because an increment of degraded insulin was not observed after dissociation. The supposition of insulin aggregates in the first peak was discarded because these insulin aggregates are not recognized by the antibody used. The strength of this interaction was important enough to require the use of chaotropic conditions for dissociation, whereas the association IDE + Insulin in degradation studies with purified IDE and insulin, could be dissociated with a pH decrease.

It was demonstrated that 10 mM ATP increased IDE hydrodynamic radius and its apparent mass (Im et al. 2007) which could be important for [IDE-Insulin] transfer to M. The big spot of insulin radioactivity during cross-linking studies could explain the conformational difficulties of IDE in mitoplasts, without counterpart in OM + IMS. The absence of radioactive insulin observed in gel autoradiography in OM + IMS would be due to the molecular distance in the pore of outer membrane translocase (TOM complex) what is the first step for mitochondrial import proteins or the speed of insulin transfer from OM to M that made ineffective the cross- linking.

We found in mitoplasts immunoblots there was a close coincidence between insulin and IDE, both detected with its specific antibodies (Fig. S5). The mechanism of protein import to mitochondria is a complex formed by the outer transporter (TOM) and the inner transporter (TIM). TOM complex formed a pore with a calculated size of 20-25 Å but TIM complex is formed by subunits being recruited during the protein import to form a charged channel with steric difficulties (Van der Laan et al. 2006; Mokranjac et al. 2005). TIM23 is an inner mitochondrial protein of 17 kDa and TIM23 complex is formed by recruitment of other proteins regulated

by the import signal of incoming preprotein during protein import to reach a complex association of 300 kDa (Mokranjac et al. 2005). Two bands of TIM23 were coincident with IDE and insulin, identified in autoradiography by the radioactive spots, but both of them with higher molecular weight of free insulin. The 136 kDa band is highly suggestive because it was increased with IDE in gel autoradiography, recognized with insulin and TIM23 antibodies in immunoblot and by its radioactive position in auto-radiographies (Fig. 6 and S5). This coincidence did not signify an association between TIM23 and IDE, though it suggested some interaction.

The ATP production is one of the main mitochondrial activities. In experimental conditions, with 1 mM of external ATP, the matrix concentration could be estimated around 7–9 mM with similar distribution in each mitochondrial compartment (Aprille 1988). ATP is an allosteric inhibitor of IDE insulin degradation, because it increases the Km (Camberos et al. 2001). Previous cross-linking studies showed that low ATP (0.5 mM) increased insulin binding to IDE, while high ATP (10 mM) produced a sharp decrease in insulin binding (Camberos & Cresto 2007). Moreover, it was shown that the enzyme was able to hydrolyze ATP, which suggested that the enzyme might modify its conformation and binding conditions (Camberos & Cresto 2007). The cytochrome b_2 had a tightly folded heme-binding domain and Glick et al. (1993) showed that high matrix ATP was required to pull into the mitochondria cytochrome b_2 with a folded heme-binding domain to insert it in IMS. The same requirement was for pb_2(1–185)-dihydrofolate reductase with a folded heme-binding domain to insert it into the mitochondrial matrix (Glick et al. 1993). This study showed the mitochondrial possibility of importing internal small folded proteins when long presequences were present in the main protein and there were high ATP levels in matrix. The same could be proposed to [insulin-IDE] complex with a long IDE presequence to be transported to mitochondrial matrix (Leissring et al. 2004; Leal et al. 2013). Moreover, the mitochondrial transfer of precursor proteins containing fold structures was proved, although they were considered to be less efficient (Schwartz et al. 1999).

In order to demonstrate that [IDE-Insulin] complex can arrive to Mx in mitoplasts and that this insulin can be released without degradation, we immunoprecipitate the IDE remaining in isolated mitoplasts. As observed in Fig. 6.3 insulin was recognize by its specific antibody in the immunoblot (intact insulin), and the ATP, previously incubated with mitochondria, did not impede the stability of [IDE-Insulin] complex until 10 mM ATP, which showed a sharp decrease of insulin bound to IDE.

Haigis et al. (2006) observed that insulin and SIRT 4 were together in mitochondria, however in these studies it was not explained how insulin arrived to mitochondria. In isolated mitochondria IDE could be used as a mitochondrial marker because it has a presequence which directs it to mitochondria (Leissring et al. 2004) and our confocal studies confirmed that insulin was colocalized with IDE. IDE had a higher mitochondrial concentration than insulin as observed in Fig. 7a, but it was dependent on many factors because we added IDE, the antibody recognize endogenous rat IDE and it is accepted that IDE has many functions in mitochondria which would require higher concentrations of IDE (Cesar Vieira et al. 2011; Udrisar et al. 2005).

We cut one mitochondrion several times and we observed the 7th section at 1.75 μm of depth that red and green were changed to yellow (merge). This change requires that both fluorescence excitations must be in the same pixel and the distance had to be less than 0.2 μm (Lachmanovich et al. 2003). In these conditions the green and red wavelengths for protein interaction discard any unspecific artifact demonstrating that free insulin, as observed before in the chromatography and immunoprecipitated IDE, was inside the mitochondrion. The antibody used only recognizes intact insulin (Camberos et al. 1982) indicating that green and yellow signify not degraded insulin. The results showing IDE-Insulin binding in OM + IMS competing with Bacitracin and the insulin accumulation in OM + IMS with low ATP concentration were coincident with mitochondrion description of green insulin in the periphery. The polar distribution of green and red color observed in Fig. 7d could mean a fast IDE-Insulin dissociation due to the high levels of ATP with mitochondrion redistribution.

The studies described here had been performed “in vitro” but animal studies showed insulin accumulation in liver and other non-pancreatic tissues (Rosenzweig et al. 1980). As described in Fig. S6, liver mitochondria accumulated “in vivo” more than 15 % of total liver insulin (100 % correction, calculated as insulin ng/g wet tissue) (Allard et al. 1952). There are many possible conditions for insulin accumulation in mitoplasts. DNP, a mitochondrial uncoupling agent, decreased the insulin transfer to M by IDE. Changes in mitochondrial energy have been proposed to be an important mechanism of enzyme activation suggesting the changes in energy as a regulator of these activities (Aprille 1988). ATP concentration could be an important factor in the insulin import to mitochondria because we observed that IDE and low ATP concentrations increases insulin in OM + IMS. Then, insulin transfer might depend on IDE-ATP hydrolysis and energy status (Aprille 1988; Glick et al. 1993). This could be applied to insulin transfer from endosomes to cytosol during insulin internalization, because the internalized insulin and its receptor were described together with IDE in endosomes (Hamel et al. 1991; Yonezawa et al. 1988).

The results showed that insulin at 25 °C were transferred from OM + IMS to mitoplasts by IDE or that the enzyme facilitates this transfer and they reach the matrix together.

Acknowledgments All authors participated in the design and interpretation of the studies, as well as in the analysis of the data and review of the work. The authors would like to thank Drs. J.J. Anderson and R. Gabach for their constant significant contribution during the development of this work and Andrea C. Cruz for her skillful help in the English revision.

References

Allard C, de Lamirande G, Cantero A (1952) Mitochondrial population in mammalian cells (liver). Cancer Res 12:580–83

Aprille JR (1988) Regulation of the mitochondrial adenine nucleotide pool size in liver: mechanism and metabolic role. FASEB J 2:2547–2556

Authier F, Bergeron JJM, Ou WJ, Rachubinski RA, Posner BI, Walton RA (1995) Degradation of the cleaved leader peptide of thiolase by a peroxisomal proteinase. Proc Natl Acad Sci U S A 92:3859–3863

Bennett RG, Hamel FG, Duckworth WC (1997) Characterization of the insulin inhibition of the peptidolytic activities of the insulin degrading enzyme-proteasome complex. Diabetes 46:197–203

Camberos MC, Cresto JC (1982) Caracterización de sueros anti-insulina para la determinación de insulina y proinsulina en pacientes. Acta Bioquim Clin Latinoam 16:453–457

Camberos MC, Cresto JC (2007) Insulin-degrading enzyme hydrolyzes ATP. Exp Biol Med 232:281–292

Camberos MC, Perez AA, Udrisar DP, Wanderley MI, Cresto JC (2001) ATP inhibits insulin-degrading enzyme activity. Exp Biol Med 226: 334–341

Caruso M, Maitan MA, Bifulco G, Miele C, Vigliotta G, Oriente F, Formisano P, Beguinot F (2001) Activation and mitochondrial translocation of protein kinase Cδ are necessary for insulin stimulation of pyruvate dehydrogenase complex activity in muscle and liver cells. J Biol Chem 276:45088–45097

César Vieira JSB, Saraiva KLA, Barbosa MCL, Porto RCC, Cresto JC, Peixoto CA, Wanderley MI, Udrisar DP (2011) Effect of dexamethasone and testosterone treatment on the regulation of insulin-degrading enzyme and cellular changes in ventral rat prostate after castration. Int J Exp Path 92:272–280

Cresto JC, Udrisar DP, Camberos MC, Basabe JC, Gomez Acuña P, de Majo SF (1981) Preparation of biologically active mono-^{125}I-insulin of high specific activity. Acta Physiol Lat 31:13–24

Duckworth WC, Bennett RG, Hamel FG (1998) Insulin degradation: progress and potential. Endocr Rev 19:608–624

Ezaki O, Kono T (1982) Effects of temperature on basal and insulin-stimulated glucose transport activities in fat cells - Further support for the translocation hypothesis on insulin action. J Biol Chem 257: 14306–14310

Glick BS, Wachter C, Reid GA, Schatz G (1993) Import of cytochrome b_2 to the mitochondrial intermembrane space: The tightly folded heme-binding domain makes import dependent upon matrix ATP. Protein Sci 2:1901–1917

Guyton AC, Hall JE: Tratado de Fisiología Humana (1997) Editor McGraw-Hill, Interamericana, Mexico Chapter 70, 961-967

Haigis MC, Mostoslavsky R, Haigis KM, Fahie K, Christodoulou DC, Murphy AJ, Valenzuela DM, Yancopoulos GD, Karow M, Blander G, Wolberger C, Prolla TA, Weindruch R, Alt FW, Guarente L (2006) SIRT4 inhibits glutamate dehydrogenase and opposes the effects of calorie restriction in pancreatic beta cells. Cell 126:941–954

Hamel FG, Mahoney MJ, Duckworth WC (1991) Degradation of intraendosomal insulin by insulin-degrading enzyme without acidification. Diabetes 40:436–443

Hamel FG, Bennet RG, Upward JL, Duckworth WC (2001) Insulin inhibits peroxisomal fatty acid oxidation in isolated rat hepatoxytes. Endocrinology 142:2702–2706

Ho YS, McKay G (1999) Pseudo-second order model for sorption processes. Process Biochem 34:451–465

Hüttemann M, Icksoo L, Samavati L, Hong Y, Doan JW (2007) Regulation of mitochondrial oxidative phosphorylation through cell signaling. Biochim Biophys Acta 1773:1701–1720

Im H, Manolopoulou M, Malito E, Shen Y, Zhao J, Neant-Fery M, Sun MS, Sisodia SS, Leissring MA, Tang WJ (2007) Structure of substrate-free human insulin-degrading enzyme (IDE) biophysical analysis of ATP-induced conformational switch of IDE. J Biol Chem 282:25453–25463

Lachmanovich E, Svartsman DE, Malka Y, Botvin C, Henis YI, Weiss AM (2003) Co-localization analysis of complex formation among membrane proteins by computerized fluorescence microscopy: application to immunofluorescence co-patching studies. J Microsc 212:122–131

Leal MC, Magnani N, Villordo S, Buslje CM, Evelson P, Castaño EM, Morelli L (2013) Transcriptional regulation of insulin-degrading enzyme modulates mitochondrial amyloid β (Aβ) peptide catabolism and functionality. J Biol Chem 288:12920–12931

Leissring MA, Farris W, Wu X, Christodoulou DC, Haigis MC, Guarente L, Selkoe DJ (2004) Alternative translation initiation generates a novel isoform of insulin-degrading enzyme targeted to mitochondria. Biochem J 383:439–446

Mokranjac D, Neupert W (2005) Protein import into mitochondria. Biochem Soc Trans 33:1019–1023

Mylotte LA, Duffy AM, Murphy M, O'Brien T, Samali A, Barry F, Szegezdi E (2008) Metabolic flexibility permits mesenchymal stem cell survival in an ischemic environment. Stem Cells 26:1325–1336

Rickwood D, Wilson MT, Darley-Usmar VM (1987) Isolation and characteristics of intact mitochondria. In: Mitochondria, a practical approach. Editor: Darley-Usmar VM, Rickwood D, Wilson MT, IRL Press Limited. Chapter 1, pp. 1-16.

Rosenzweig JL, Havrankova J, Lesniak MA, Brownstein M, Roth J (1980) Insulin is ubiquitous in extra-pancreatic tissues of rats and humans. Proc Natl Acad Sci U S A 77:572–576

Salvi M, Brunati AM, Toninello A (2005) Tyrosine phosphorylation in mitochondria: a new frontier in mitochondrial signaling. Free Radic Biol Med 38:1267–1277

Schwartz MP, Huang S, Matouschek A (1999) The structure of precursor proteins during import into mitochondria. J Biol Chem 274:12759–12764

Udrisar DP, Wanderley MI, Porto RCC, Cardoso CLP, Barbosa CL, Camberos MC, Cresto JC (2005) Androgen and androgen-dependent regulation of insulin-degrading enzyme in subcellular fractions of rat prostate and uterus. Exp Biol Med 230: 479–487

Van der Laan M, Rissier M, Rehling P (2006) Mitochondrial pre-protein translocases as dynamic molecular machines. FEMS Yeast Res 6: 849–861

Wymann M, Bulgarelli-keva G, Zvelebil MJ, Pirola L, Vanhaesebroeck B, Waterfield D, Panayotou G (1996) Wortmannin inactivates phosphoinositide 3-kinase by covalent modification of Lys-802, a residue involved in the phosphate transfer reaction. Mol Cel Biol 16: 1722–1733

Yonezawa K, Yokono K, Shii K, Hari J, Yaso S, Amano K, Sakamoto T, Kawase Y, Akiyama H, Nagata M, Baba S (1988) Insulin-degrading enzyme is capable of degrading receptor-bound insulin. Biochem Biophys Res Commun 150:605–614